Korean J. Chem. Eng., 34(5), 1483-1489 (2017)
DOI: 10.1007/s11814-017-0023-3

pISSN: 0256-1115
eISSN: 1975-7220

Effect of electrolyte composition on the morphological structures of dendritic copper powders prepared by a spontaneous galvanic displacement reaction

Kai Zhuo*, Chang Yong An*, Padmanathan Karthick Kannan*, Nary Seo*, Yu-Seon Park*, and Chan-Hwa Chung*,,†**

*School of Chemical Engineering, Sungkyunkwan University, Suwon 16419, Korea
**Farad Materials, Co., Ltd., Suwon 16419, Korea
(*Received 19 October 2016 • accepted 6 February 2017*)

Abstract−Dendritic copper powders are highly desirable in many applications, including electromagnetic interference shielding and conductive pastes, because of low cost and high conductivity. We prepared dendritic copper powders using the galvanic displacement reaction between the Al and Cu-ions in aqueous solution. This method is very simple and spontaneous at room temperature. During the process, the morphology of the copper powders is strongly affected by several variables, such as the displacement reaction rate and the amount of hydrogen evolution due to the reduction of proton. The effect of the different composition of electrolytes to morphological changes of copper powders was investigated in this study. In addition, the effects of concentration of chlorine ion, pH, termination time, and additives were monitored, which resulted in different morphology. Considering different applications, such as sensors, catalysts, and conductive pastes, the controllability of the morphology of dendritic copper powders plays an important role in achieving high performance in desired applications.

Keywords: Dendritic Copper Powders, Galvanic Displacement Reaction, Morphology, Hydrogen Bubbles, Copper Complex, Reduction Potential

INTRODUCTION

In many industrial applications, the metal powders of silver, gold, platinum, palladium, nickel, copper, and aluminum, are used as a conductive matter, an adsorbed substrate, a catalytic surface, or an electrode. Over the past few decades, the rapid development of the miniaturization of electronic components has been realized in the electronics, information, and communications industries. To meet these criteria, the applications of chip-based and multi-layered processes are preferred; conductive metal powders such as silver, copper, nickel, and aluminum are widely used in the production of electronic slurries (conductive pastes and adhesives) or conductive films.

These electronic slurries are used to build electrodes with resistors, capacitors, inductors, sensors, and current collectors. Due to the superior value of the electrical conductivity, the silver slurry or paste is predominantly used in the electronic printing market [1-11]. Silver powders have been fabricated by different methods including a galvanic displacement reaction (GDR) on zinc [12-16], copper [17-20], or aluminum metal surfaces [18,21,22]. However, there has always been a search for alternative materials with similar property because of the high cost of silver powders. Recently, as an alternative to silver, silver-coated copper powders with core-shell structures are considered as an alternative because of their high conductivity as equivalent to silver with very low cost [1,3,23-38]. Copper powders have already been used in many applications due to their catalytic, optical, and conducting properties. Additionally, copper is relatively cheap (about one percent of the silver price) and has a high electrical conductivity (only about 6% less than that of silver). Copper materials have been prepared by electro-deposition [39-41], electroless deposition [42-44], hydrothermal treatment [45-47], and a galvanic displacement reaction [2,48]. Upon being exposed to air, however, copper is extremely unstable and easily oxidized, even at room temperature. By taking the advantage of the high conductivity of silver paste, a copper surface covered with a layer of silver has received great attention [1,3,23-38,49,50].

It is well known that the morphology of metal powders plays an important role in achieving high performance in most technological applications, which is the reason why many researches undergo not only on the search for the alternative materials but also the control of the particle shape. Recently, several copper-based materials with different morphologies have been studied in the form of spherical structure, wires, and dendrites. Among these structures, dendrites have a hierarchical structure consisting of a stem and many branches, which results in large surface area to volume ratio. In most of the cases, the lager surface area of the metal provides the better performance in the applications. Dendritic materials have been fabricated by several electrochemical processes in aqueous electrolyte such as electro-plating, electroless deposition, and galvanic displacement reaction. Using the electro-plating process accompanied with hydrogen evolution reaction, Shin et al. synthesized porous dendritic tin and copper layer as a film on the conductive substrate [51]. In some earlier reports, the dendritic Ag nanostructures were prepared by a galvanic displacement reaction using zinc metals [40,44].

†To whom correspondence should be addressed.
E-mail: chchung@skku.edu

In this work, dendritic copper powders were prepared by the galvanic displacement reaction without any reducing agents, and the changes in morphology were examined by varying the chemical composition of the electrolyte. Especially, the effects of pH, halide-ion concentration, and additives on the change in morphology of dendritic structures were studied.

EXPERIMENTAL

High purity (99.9%) aluminum foil (7×8 cm^2) was treated in 1 M NaOH electrolyte for 5 minutes to remove the native oxide and was carefully cleaned with deionized water. Copper chloride dehydrate ($CuCl_2 \cdot 2H_2O$) or copper sulfate pentahydrate ($CuSO_4 \cdot 5H_2O$) was dissolved in 500 ml of de-ionized (DI) water as a source of copper ion, and the pH of the electrolyte was adjusted by adding the sulphuric acid (H_2SO_4) or hydrochloric acid (HCl) into the electrolyte. Some other salts and additives were also added to the electrolytes to determine their effect on the morphological changes of dendritic structures. All the chemicals were purchased from Sigma-Aldrich, and more detailed compositions of the electrolytes were listed in Table 1.

Once the electrolyte was prepared, the pre-cleaned aluminium foil was immersed into the electrolyte at room temperature for 5-20 minutes. The as-prepared dendritic copper powders were separated from the slurry and washed several times with DI water and ethanol to ensure that the impurities were completely removed. The cleaned copper powders were dried in vacuum oven at 60 °C for12 hours for further analysis.

The structures and morphologies of the dendritic copper powders were monitored by the field-emission scanning electron microscopy (FESEM, JEOL, JSM7000F). The composition, chemical state, and crystallinity of the powders were examined using x-ray diffraction (XRD, Bruker, D8 ADVANCE).

To evaluate the conductivity of the obtained powders, 0.2 g dendritic copper powders were pelletized under the pressure of 10 MPa. The resistivity of copper powders was measured by the 4-point probe method. The resistance value was recorded at a constant current of 20 μA by using current source (Keithley 6221) and a nanovoltmeter (Keithley 2182A), when a probe was produced with tungsten and the distance between the probes was 1 mm.

RESULTS AND DISCUSSION

The galvanic displacement reaction (GDR) between Al and Cu^{2+} ions in acidic aqueous electrolytes of H_2SO_4 or HCl, provides a remarkably simple and versatile route for the preparation of dendritic Cu powders, as shown in Fig. 1 and Fig. 2. The key step of this process involves the replacement reaction between a suspension of metal templates and a salt precursor containing a relatively less active metal. The bubbles and voids, generated by hydrogen evolution reaction during the reduction of copper-ions by the GDR, establish the casting frame for dendritic Cu growth [52]. The copper powders were obtained from the GDR process, of which reaction is driven by the difference between the reduction potentials of Al and Cu ions in the electrolyte. Because the reduction potential of Al is −1.68 V and that of Cu is +0.34 V, the copper has to be reduced and aluminium to be ionized into the electrolyte. At the same time, considering the reduction potential of proton is +0.0 V by definition, the hydrogen is produced by reduction of proton at the surface of Al as follows:

$$2Cu^{2+}+2H^{+}+2Al(s)\rightarrow 2Cu(s)+H_2(g)+2Al^{3+} \quad (1)$$

1. Effect of Cl^-

The copper ions are actually in the form of blue-colored [Cu

Table 1. The stem length and relationship between stem and branches

Electrolytes	L_1 (μm)	L_2/L_1	L_3/L_2
0.01 M $CuCl_2$	4.2	25.00%	0.00%
0.1 M $CuCl_2$	3.9	12.50%	0.00%
0.1 M $CuCl_2$ 0.01 M NaCl	4	14.29%	0.00%
0.1 M $CuCl_2$ 0.1 M NaCl	6.5	20.00%	10.00%
0.1 M $CuCl_2$ 1 M NaCl	7	25.00%	15.00%
2 M H_2SO_4 0.1 M $CuCl_2$	1.6	0.08%	0.00%
1 M H_2SO_4 0.1 M $CuCl_2$	4.5	27.27%	0.00%
0.5 M H_2SO_4 0.1 M $CuCl_2$	8.6	20.00%	0.00%
0.1 M H_2SO_4 0.1 M $CuCl_2$	10	18.87%	0.00%
0.5 M H_2SO_4 0.1 M $CuSO_4$ 0.1 M KCl	30	5.26%	0.00%
0.5 M H_2SO_4 0.1 M $CuSO_4$ 0.1 M NaCl	30	3.85%	0.00%
0.5 M H_2SO_4 0.1 M $CuSO_4$ 0.1 M KBr	100	20.00%	20.00%
0.5 M H_2SO_4 0.1 M $CuSO_4$ 0.1 M NaBr	100	20.00%	12.50%
0.5 M H_2SO_4 0.1 M $CuCl_2$ (5 min)	5	21.74%	0.00%
0.5 M H_2SO_4 0.1 M $CuCl_2$ (10 min)	7	20.00%	0.00%
0.5 M H_2SO_4 0.1 M $CuCl_2$ (15 min)	9	15.15%	0.00%
0.5 M H_2SO_4 0.1 M $CuCl_2$ (20 min)	9.3	12.50%	0.00%
0.5 M H_2SO_4 0.1 M $CuCl_2$ 0.3 M sodium citrate	50	20.00%	40.00%
0.5 M H_2SO_4 0.1 M $CuSO_4$ 0.1 M CTAB	80	1.89%	0.00%

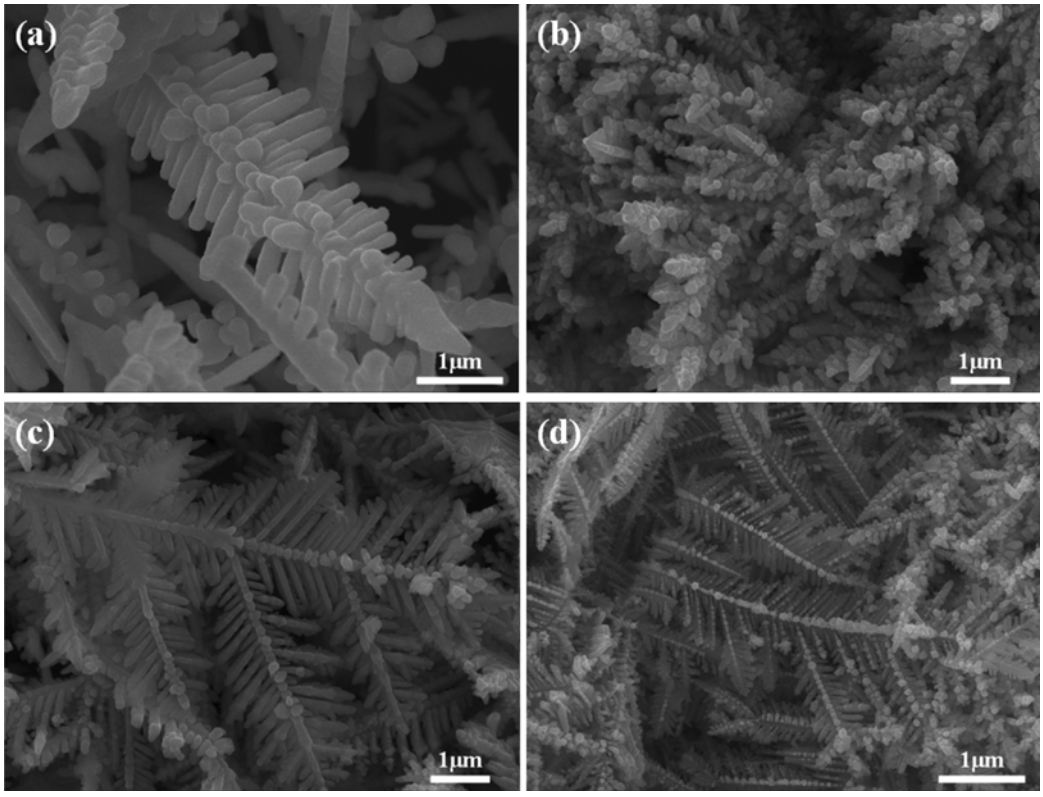

Fig. 1. FE-SEM images of dendritic copper powders obtained in electrolytes (a) 0.1 M $CuCl_2$, (b) 0.1 M $CuCl_2$, 0.01 M NaCl, (c) 0.1 M $CuCl_2$, 0.1 M NaCl, and (d) 0.1 M $CuCl_2$, 1 M NaCl, respectively.

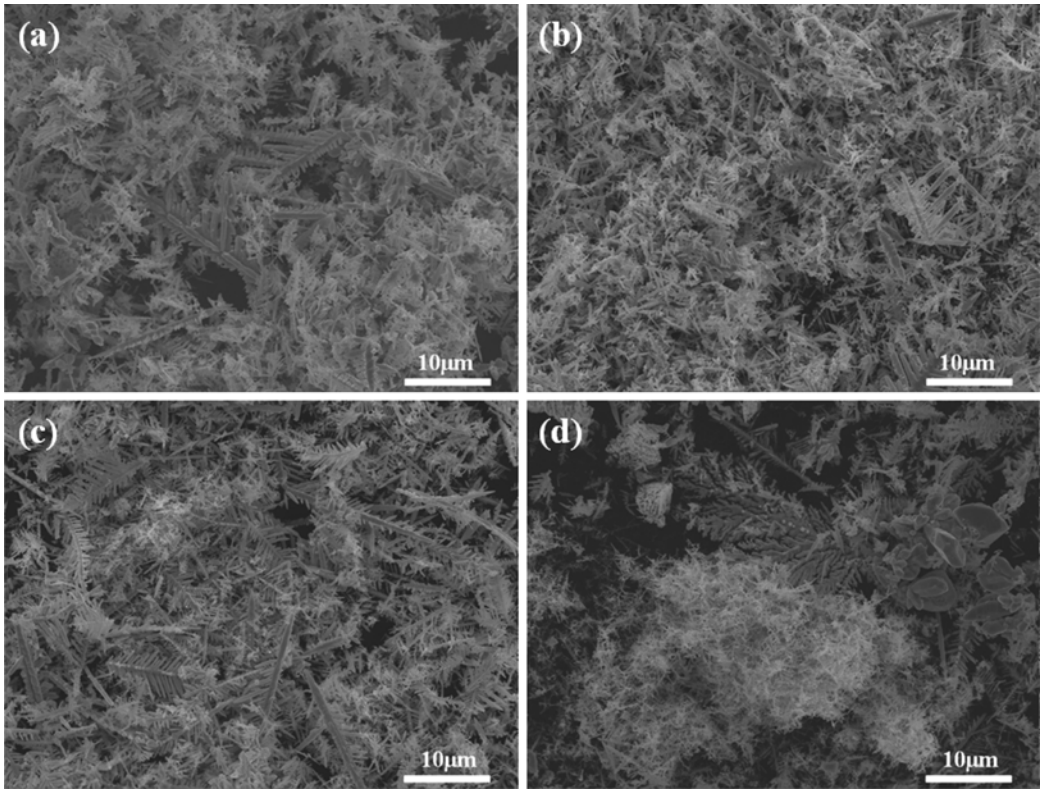

Fig. 2. FE-SEM images of dendritic copper powders obtained in electrolytes (a) 2 M H_2SO_4, 0.1 M $CuCl_2$, (b) 1 M H_2SO_4, 0.1 M $CuCl_2$, (c) 0.5 M H_2SO_4, 0.1 M $CuCl_2$, and (d) 0.1 M H_2SO_4, 0.1 M $CuCl_2$, respectively.

$(H_2O)_6]^{2+}$ in aqueous solution [53]. Control of the Cl^- ion concentration is an important factor in the galvanic displacement reaction. The chloride ions were found to cause hydrogen bubble generation and a fast displacement reaction in the case of Ni-Cu powders [52]. When the aluminium foil is immersed into the electrolyte consisting of $CuSO_4$ or $CuSO_4$ with H_2SO_4, even after 24 hr, there were no copper powders and hydrogen bubbles. However, after the addition of NaCl or HCl with the above two electrolytes, the $[Cu(H_2O)_6]^{2+}$ was converted to other form as $[CuCl_4]^{2-}$ [53]. As a result, bubbles were generated on the surface of aluminium with bright red powders on the surface of aluminium foil according to the following reactions:

$$3[CuCl_4]^{2-}+2Al(s)\rightarrow 3Cu(s)+12Cl^-+2Al^{3+} \quad (2)$$

$$6H^++2Al(s)\rightarrow 2Al^{3+}+3H_2(g) \quad (3)$$

In view of the above phenomenon, a series of experiments were performed to find the role of chloride ions. Additionally, chloride ions also influence the morphology of copper powders, as shown in Fig. 1. The first branch appeared in electrolyte containing 0.1 M $CuCl_2{\cdot}6H_2O$ (*cf.* Fig. 1(a)) and the growth of branches proceeded toward four perpendicular directions around the stem. The second and third branches were generated with higher concentrations of Cl^- by adding more NaCl (*cf.* Fig. 1(c) and (d)). At the same time, the direction of growth changed within the same plane as the stem. In aqueous solution, $[Cu(H_2O)_6]^{2+}$ was transformed to $[CuCl_4]^{2-}$ because the bonding energy of Cu-O is lower than Cu-Cl. As mentioned in Eqs. (2) and (3), Al acting as a reducing agent in the GDR, which replaces the Cu^{2+} in $[CuCl_4]^{2-}$ more difficultly than Cu^{2+} in $[Cu(H_2O)_6]^{2+}$, while the hydrogen bubbles are generated continuously. When the electrolyte contains a high concentration of chlorine ions, the settlement of the displaced copper atoms transferred from the solution to the ionic metal lattice is limited by the hydrogen evolution. The growth of copper was chopped by the relatively abundant amount of hydrogen bubbles, which resulted in small branches with high concentration of chloride ions. The lengths of stem, first branch, and second branch were marked as L_1, L_2, and L_3, respectively. The L_1/L_2 ratio decreased as the concentration of Cl^- was increased.

2. Effect of H^+

To demonstrate the effect of hydrogen ions on the morphology of dendritic copper powders, the 500 ml aqueous solutions containing 0.1 M $CuCl_2$ with different concentration of H_2SO_4 viz. 0.1 M, 0.5 M, 1 M, and 2 M were prepared and investigated. It can be observed that more hydrogen bubbles were generated with increase in H^+ concentrations. As shown in Fig. 2(a), the amount of hydrogen evolution was too high to assist in forming long stems of dendritic copper from copper ions. On the other hand, with low H^+ concentrations, the amount of hydrogen evolution was too low, which actually affected the uniformity in the formation dendritic copper powders (*cf.* Fig. 2(d)). Fig. 2(c) shows that the nano-branched copper powders were uniform with an average stem length of 8 μm.

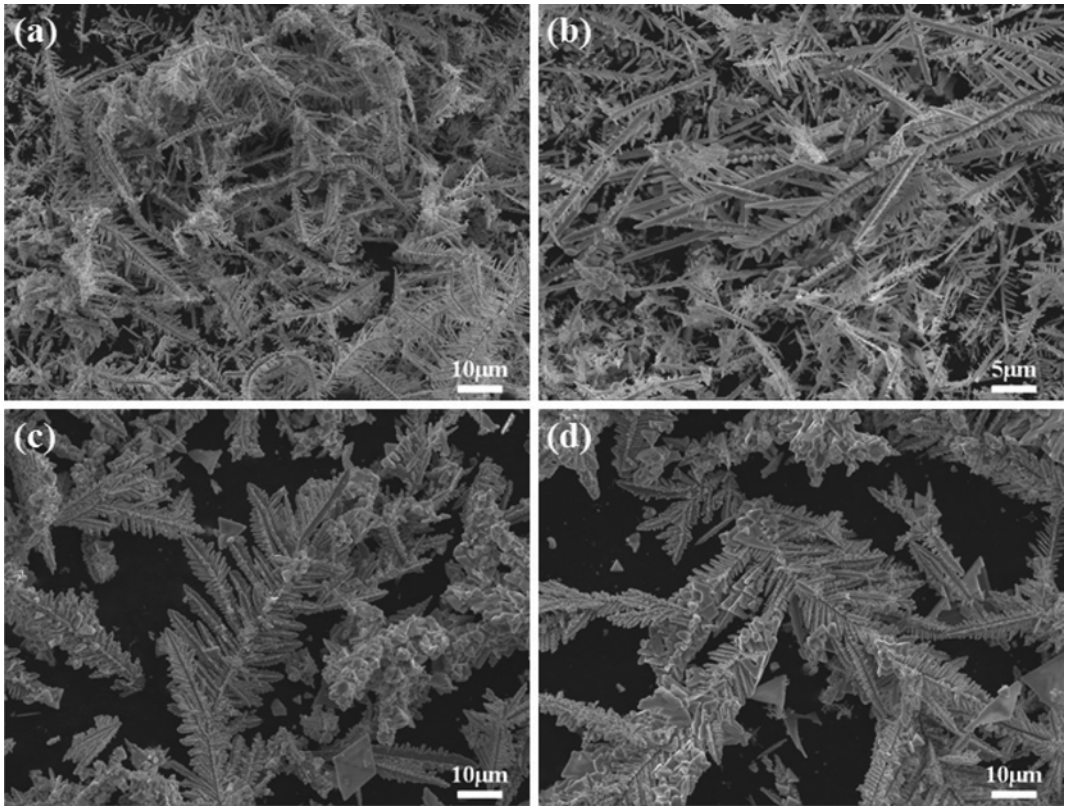

Fig. 3. FE-SEM images of dendritic copper powders obtained in electrolytes (a) 0.5 M H_2SO_4, 0.1 M $CuSO_4$ and 0.1 M KCl, (b) 0.5 M H_2SO_4, 0.1 M $CuSO_4$ and 0.1 M NaCl, (c) 0.5 M H_2SO_4, 0.1 M $CuSO_4$ and 0.1 M KBr, and (d) 0.5 M H_2SO_4, 0.1 M $CuSO_4$ and 0.1 M NaBr, respectively.

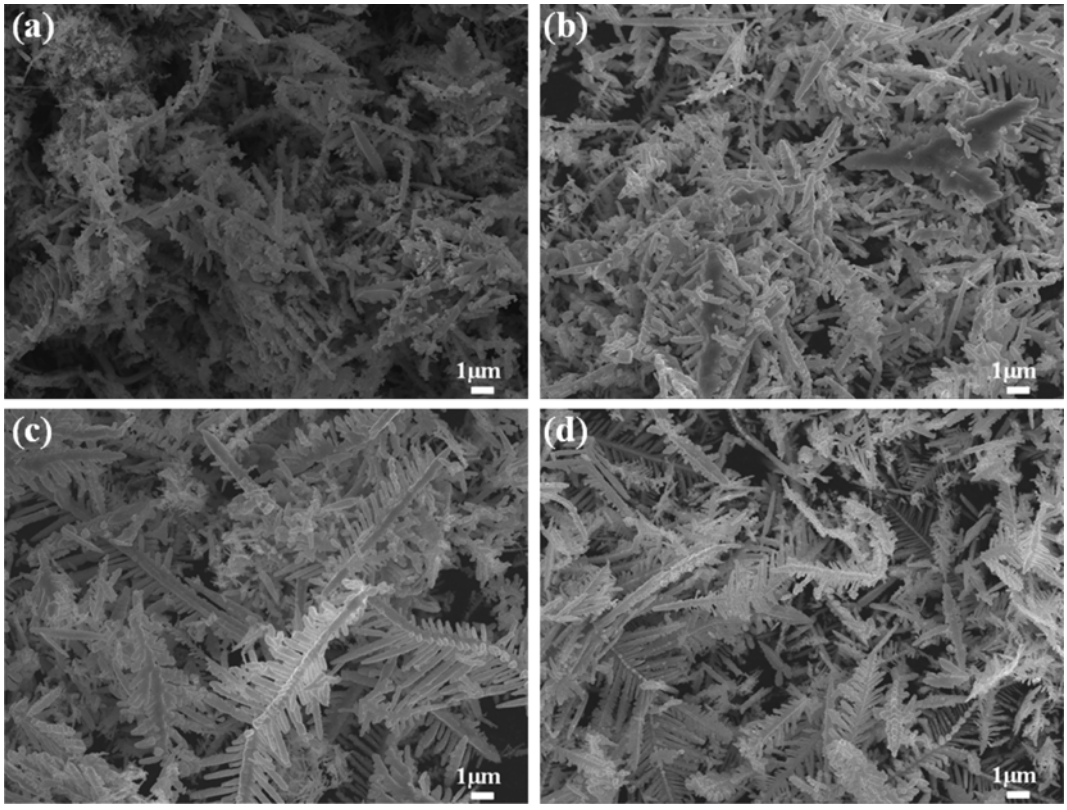

Fig. 4. Time-dependent evolution of branched copper powders at different growth stage: (a) 5 min, (b) 10 min, (c) 15 min, and (d) 20 min obtained in electrolyte containing 0.5 M H_2SO_4 and 0.1 M $CuCl_2$.

3. Effect of Halide Ions

In Fig. 3, the morphology of copper obtained from 0.5 M H_2SO_4, 0.1 M $CuSO_4$, and 0.1 M KCl (*cf.* Fig. 3(a)) was similar to that obtained from 0.5 M H_2SO_4, 0.1 M $CuSO_4$, and 0.1 M NaCl (*cf.* Fig. 3(b)). The same phenomenon was found in electrolytes consisting of 0.5 M H_2SO_4, 0.1 M $CuSO_4$, 0.1 M KBr (*cf.* Fig. 3(c)), and 0.5 M H_2SO_4, 0.1 M $CuSO_4$, and 0.1 M KBr (*cf.* Fig. 3(a)). Fig. 3(a) and 3(b) indicate that the stem growth was very long, but the branches were only in the nano-meter scale. The copper powders fabricated from electrolyte including Br^- had thick stems and branches compared to Cl^-. The third branches were also formed.

4. Effect of the Termination Time

Fig. 4 presents the time-dependent evolution of branched copper powders at different growth stages, (a) 5 min, (b) 10 min, (c) 15 min, and (d) 20 min, obtained in electrolyte containing 0.5 M H_2SO_4 and 0.1 M $CuCl_2$. From 5 min to 15 min, the dendrite kept growing at a rate of 2-3 μm/min. However, when the termination time reached more after 20 min, not much difference in the length of dendrite was monitored. It can be considered that the copper ions were almost depleted by the reaction within 15 min, which resulted in a shortage of the amount of copper ions to support the further growth of copper dendrites.

5. Effect of Additives

Adsorbed additives affect the kinetics of copper deposition and the growth mechanism by changing the concentration of growth sites on a surface, the concentration of ions on the surface, the diffusion coefficient, and the activation energy of surface diffusion of adsorbed ions. In the presence of adsorbed additives, the mean free-path for lateral diffusion of adsorbed ions was diminished, which is equivalent to a decrease in the diffusion coefficient (diffusivity) of adsorbed ions. This decrease in diffusion coefficient may result in an increase in adsorbed ion concentration at steady state, and thus an increase in the frequency of the two-dimensional nucleation between diffusing adsorbed-ions. Additives can also influence the propagation of micro-steps and cause bunching and the formation of macro-steps. For example, in the electrodeposited film, the structure and morphology of the surface depend on the surface coverage of additives [54].

In this work, the additives also play an important role in the control of morphology of dendritic copper powders. The Cu powders generated with 0.5 M H_2SO_4, 0.1 M $CuCl_2$, and the additive of 0.3 M sodium citrate are shown in Fig. 5(a) and (b). The growth direction of the branches scattered at an oblique angle from the stem. The size of the dendrite was about 50 μm. When using the additive of 0.1 M CTAB instead of 0.3 M sodium citrate, the branches with about a length of 1 μm tilted in a straight line arrangement (*cf.* Fig. 5(c) and (d)) with a size greater than 80 μm. The additives changed the direction of growth and enlarged the size of the dendrite by more than a factor of 10.

The relationship between the lengths of the stem and branch was analyzed and the results shown in Table 1. The size of the copper dendrites was controlled except when adding additives or a large amount of Cl^-. The ratio of L_2 to L_1 decreased as the concentration of Cl^- was increased and stabilized at the termination time.

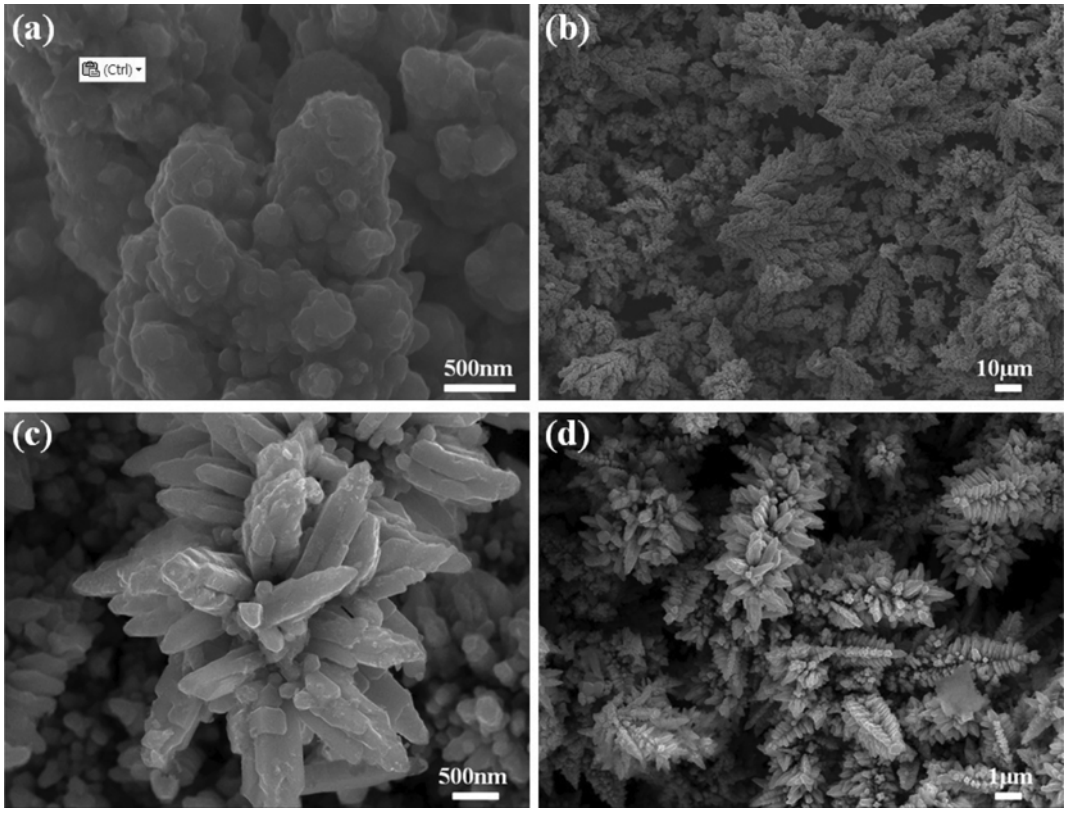

Fig. 5. FE-SEM images of dendritic copper powders prepared in (a) (b) 0.5 M H_2SO_4, 0.1 M $CuCl_2$ and 0.3 M sodium citrate, (c) (d) 0.5 M H_2SO_4, 0.1 M $CuSO_4$ and 0.1 M CTAB, respectively.

The third branches only appeared under certain conditions when the additives were added. The concentrations of Cl^- and H^+ simultaneously controlled the morphology and dendrite size as well. The size of copper dendrites was controlled in the range of 5-10 μm by using different amounts of Cl^- and H^+ in copper electrolytes.

The conductivity was evaluated by the measurement of bulk resistance of pelletized powders. The measured resistance value with the 4-point probe was converted into resistivity according to Pouillet's law as in the following equation:

$$R = \rho \frac{L}{w \cdot t} \quad (4)$$

where ρ is bulk resistivity, R is resistance measured with the 4-point probe, and L, w, and t is length, width, and thickness of the pellet, respectively.

In this work, the typical resistivity of dendritic copper powders was measured to 0.74 μΩ·m, of which value was fairly low resistivity that can be used as a metallic filler in the conductive paste.

SUMMARY

We developed a simple method for the preparation of copper powders with a dendritic morphology at a low temperature. To optimize the dendritic structures, the galvanic displacement reaction and hydrogen evolution reactions were employed simultaneously. The formation mechanism of the copper dendritic structures was studied as functions of the concentration, termination time, an ion concentration, and the addition of additives.

ACKNOWLEDGEMENTS

This work was supported by the Basic Science Research Program of the National Research Foundation of Korea (NRF) funded by grants from the Ministry of Science, ICT, and Future Planning (NRF-2016R1A2A2A05005327), and the Strategic Core Materials Technology Development Program (10047681, Development of Low-Cost Conductive Paste Capable of Fine Pattern for Touch Panel and High Conductivity for Solar Cell Using Metal Composite with Core-Shell Structure Prepared by Highly-Productive Wet Process) funded by the Ministry of Trade, Industry & Energy (MI, Korea).

REFERENCES

1. C. K. Kim, G.-J. Lee, M. K. Lee and C. K. Rhee, *Powder Technol.*, **263**, 1 (2014).
2. X. G. Cao and H. Y. Zhang, *Electron. Mater. Lett.*, **8**(4), 467 (2012).
3. R. Zhang, W. Lin, K. Lawrence and C. P. Wong, *Int. J. Adhes. Adhes.*, **30**, 403 (2010).
4. H. T. Hai, H. Takamura and J. Koike, *J. Alloy. Compd.*, **564**, 71 (2013).
5. M. Wu, B. Lin, Y. Cao, J. Song, Y. Sun, H. Yang and X. Zhang, *J. Mater. Sci.-Mater. El.*, **24**, 4913 (2013).
6. I. Khatri, A. Hoshino, F. Watanabe, Q. Liu, R. Ishikawa, K. Ueno and H. Shirai, *Thin Solid Films*, **558**, 306 (2014).

7. M. Theuring, M. Vehse, K. Maydell and C. Agert, *Thin Solid Films*, **558**, 294 (2014).
8. H. Nishikawa, S. Mikami, K. Miyake, A. Aoki and T. Takemoto, *Mater. Trans.*, **51**(10), 1785 (2010).
9. Z. Chen, X. Zhang, J. Fang, J. Liang, X. Liang, J. Sun, D. Zhang, N. Wang, H. Zhao, X. Chen, Q. Huang, C. Wei and Y. Zhao, *Appl. Energy*, **135**, 158 (2014).
10. T. L. Yang, K. Y. Huang, S. Yang, H. H. Hsieh and C. R. Kao, *Sol. Energy Mat. Sol. C.*, **123**, 139 (2014).
11. J.-T. Tsai and S.-T. Lin, *J. Alloy. Compd.*, **548**, 105 (2013).
12. X. Wen, Y.-T. Xie, M. W. C. Mak, K. Y. Cheung, X. Li, R. Renneberg and S. Yang, *Langmuir*, **22**, 4836 (2006).
13. J. Fang, H. You, P. Kong, Y. Yi, X. Song and B. Ding, *Cryst. Growth Des.*, **7**(5), 864 (2007).
14. S. Lv, H. Suo, X. Zhao, C. Wang, S. Jing, T. Zhou, Y. Xu and C. Zhao, *Solid State Commun.*, **149**, 1755 (2009).
15. S. Lu, H. Suo, H. Wang, C. Wang, J. Wang, Y. Xu and C. Zhao, *Solid State Sci.*, **12**, 1287 (2010).
16. S. Lu, H. Suo, T. Zhou, C. Wang, S. Jing, Q. Fu, Y. Xu and C. Zhao, *Solid State Commun.*, **149**, 227 (2009).
17. J. R. Kramer, N. H. Werstiuk and B. Ni, *J. Phys. Chem. A*, **110**, 273 (2006).
18. Y. Zhuo, W. Sun, L. Dong and Y. Chu, *Appl. Surf. Sci.*, **257**, 10395 (2011).
19. R. Liu and A. Sen, *Chem. Mater.*, **24**, 48 (2012).
20. X. Chen, C.-H. Cui, Z. Guo, J.-H. Liu, X.-J. Huang and S.-H. Yu, *Small*, **7**(7), 858 (2011).
21. R. Liu, S. Li, X. Yu, G. Zhang, Y. Ma, J. Yao, B. Keita and L. Nadjo, *Cryst. Growth Des.*, **11**, 3424 (2011).
22. T.-K. Huang, T.-H. Cheng, M.-Y. Yen, W.-H. Hsiao, L.-S. Wang, F.-R. Chen, J.-J. Kai, C.-Y. Lee and H.-T. Chiu, *Langmuir*, **23**, 5722 (2007).
23. M. N. Nadagouda and R. S. Varma, *Crys. Growth Des.*, **7**(12), 2582 (2007).
24. D. S. Jung, H. M. Lee, Y. C. Kang and S. B. Park, *J. Colloid Interface Sci.*, **364**, 574 (2011).
25. H. T. Hai, J. G. Ahn, D. J. Kim, J. R. Lee, H. S. Chung and C. O. Kim, *Surf. Coat. Technol.*, **201**, 3788 (2006).
26. X. Xu, X. Luo, H. Zhuang, W. Li and B. Zhang, *Mater. Lett.*, **57**, 3987 (2003).
27. G. Barcaro, A. Fortunelli, G. Rossi, F. Nita and R. Ferrando, *J. Phys. Chem. B.*, **110**, 23197 (2006).
28. X. G. Cao and H. Y. Zhang, *Electron. Mater. Lett.*, **8**(4), 467 (2012).
29. J. Zhao, D. Zhang and J. Zhao, *J. Solid State Chem.*, **184**, 2339 (2011).
30. X. G. Cao and H. Y. Zhang, *Appl. Surf. Sci.*, **264**, 756 (2013).
31. H. T. Hai, H. Takamura and J. Koike, *J. Alloy Compd.*, **564**, 71 (2013).
32. M. Wu, B. Lin, Y. Cao, J. Song, Y. Sun, H. Yang and X. Zhang, *J. Mater. Sci.-Mater. Electron.*, **24**, 4913 (2013).
33. Y. Kang and F. Chen, *J. Appl. Electrochem.*, **43**, 667 (2013).
34. K. Chen, D. Ray, Y. Peng and Y. Hsu, *Curr. Appl. Phys.*, **13**, 1496 (2013).
35. X. G. Cao and H. Y. Zhang, *Powder Technol.*, **226**, 53 (2012).
36. J. Zhao, D. Zhang and X. Song, *Appl. Surf. Sci.*, **258**, 7430 (2012).
37. V. Mancier, C. R. Bertrand, J. Dille, J. Michel and P. Fricoteaux, *Ultrason. Sonochem.*, **17**, 690 (2010).
38. C.-H. Tsai, S.-Y. Chen, J.-M. Song, I.-G. Chen and H.-Y. Lee, *Corros. Sci.*, **74**, 123 (2013).
39. S. Cherevko and C.-H. Chung, *Talanta*, **80**, 1371 (2010).
40. S. Arai and T. Kitamura, *ECS Electrochem. Lett.*, **3**(5), D7 (2014).
41. R. Qiu, H. G. Cha, H. B. Noh, Y. B. Shim, X. L. Zhang, R. Qiao, D. Zhang, Y. I. Kim, U. Pal and Y. S. Kang, *J. Phys. Chem. C*, **113**, 15891 (2009).
42. S. S. Djokić and N. S. Djokić, *J. Electrochem. Soc.*, **158**(4), D204 (2011).
43. S.-H. Wu and D.-H. Chen, *J. Colloid Interface Sci.*, **273**, 165 (2004).
44. C. Yan and D. Xue, *Cryst. Growth Des.*, **8**(6), 1849 (2008).
45. Y. Liu, Y. Chu, Y. Zhuo, L. Dong, L. Li and M. Li, *Adv. Funct. Mater.*, **17**, 933 (2007).
46. X. Zhang, G. Wang, X. Liu, H. Wu and B. Fang, *Cryst. Growth Des.*, **4**, 1430 (2008).
47. Z. Y. Zhang, C. G. Hu, B. Feng, C. H. Zheng, X. S. He and X. Wang, *J. Supercond. Nov. Magn.*, **23**, 893 (2010).
48. S. Mahima, C. Karthik, S. Garg, R. Mehta, R. Teki, N. Ravishankar and G. Ramanath, *Cryst. Growth Des.*, **10**, 3925 (2010).
49. Y. Zeng, T. Li, M. Fu, S. Jiang and G. Zhang, *J. Alloy. Compd.*, **585**, 277 (2014).
50. L.-M. Huang, L.-M. Luo, X.-Y. Ding, G.-N. Luo, X. Zan, J.-G. Cheng and Y.-C. Wu, *Powder Technol.*, **258**, 216 (2014).
51. H. C. Shin, J. Dong and M. Liu, *Adv. Mater.*, **15**(19), 1610 (2003).
52. K. Zhuo, M.-G. Jeong and C.-H. Chung, *RSC Adv.*, **3**, 12611 (2013).
53. P. L. Soni and Vandna Soni, Coordination Chemistry, Taylor & Francis Group, Boca Raton, FL (2013).
54. M. Schlesinger and M. Paunovic, Modern electroplating, New York, Wiley, 5th Ed. (2010).